Finite Element Stress Analysis of the CMS Magnet Coil

A. Desirelli*, P. Fabbricatore†, S. Farinon†, B.Levesy††,C. Ps††, J.M. Rey††, S.Sgobba*

*C.E.R.N., European Organisation for Nuclear Research, Geneva, Switzerland
†I.N.F.N. - Genova, Istituto Nazionale di Fisica Nucleare, Genova, Italy
††C.E.A.-Saclay, Gif-sur-Yvette, France

***Abstract*-- The Compact Muon Solenoid (CMS) is one of the experiments which are being designed in the framework of the Large Hadron Collider (LHC) project at C.E.R.N. The design field of the CMS magnet is 4 T, the magnetic length is 12.48 m and the aperture is 6.36 m. This is achieved with a 4 layer-5 module superconducting Al-stabilized coil energised at a nominal current of 20 kA. The finite element analysis (FEA) carried out is axisymmetric elasto-plastic. FEA has also been carried out on the suspension system and on the conductor.**

I. Introduction

The Compact Muon Solenoid (CMS) is one of the experiments which are being designed in the framework of the Large Hadron Collider (LHC) project at C.E.R.N. The design field of the CMS magnet is 4 T, the magnetic length is 12.48 m and the aperture is 6.36 m [1]. This is achieved with a 4 layer-5 module superconducting Al-stabilized coil energised at a nominal current of 20 kA. One of the features of the CMS magnet is the partially self-supporting character of the winding. In this coil the structural function is ensured, unlike in other existing Al-stabilized thin solenoids, partly by the Al-alloy reinforced conductor and partly by the external former. Elasto-plastic axisymmetric FEA has been carried out at C.E.A.-Saclay and I.N.F.N.-Genova using two different FE codes (ANSYS and CASTEM). Details on the cross section of the conductor and the four layer winding can be found in [1] and [2].

II. The FE Model

The coil has been simulated with an elasto-plastic axisymmetric FE model. A sub-modelling technique was used for the FEA due to the size of the problem and its non linearity due to the plastic flow of pure Al. Two locations: coil end and coil centre were chosen for the sub-modelling. Each sub-model comprises 4 layers and 8 turns. Several sub-models for different locations and different degrees of detail have been run. No major differences have been found between the stress distributions of the aligned turn and the staggered turn sub-models (see Fig. 1). The results presented here are those of the sub-model with aligned turns. The stress analysis has been carried out, both for nominal and keystoned cable geometry, .for two main operating conditions:
- coil at 4.5 K,
- coil at 4.5 K energised (19.5 kA).

The real load history of the coil, during cool down and energisation, should be taken into account as the problem is non-conservative (i.e. history dependant) due to the plastic flow of pure Al. However, for this analysis, one single load step both for cool down and energisation has been used. This is a fair approximation if one assumes monotonic cooling and energisation.

A. Modelling of the Pure Al-Stabilizer

The pure Al has been modelled as elasto-plastic isotropic material with Von Mises yield criterion and kinematic hardening rule. Fig. 2 shows the experimental stress strain curve, measured at 4.2 K, of pure Al (fully annealed) of the Aleph conductor [3].

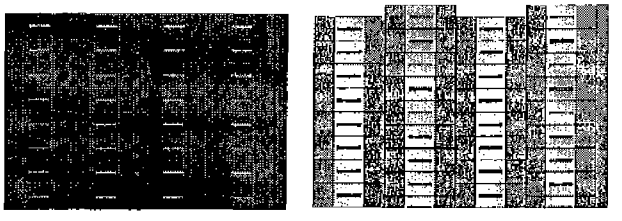

Fig. 1. Sub-models with aligned and staggered turns.

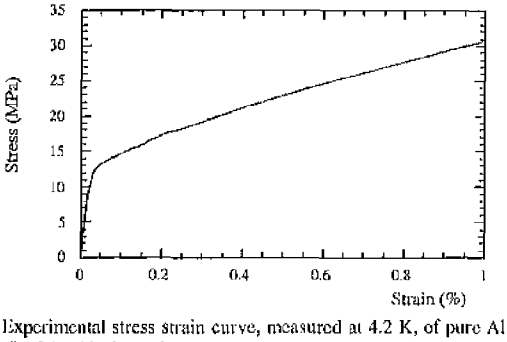

Fig. 2. Experimental stress strain curve, measured at 4.2 K, of pure Al (fully annealed) of the Aleph conductor.

Manuscript received September 27, 1999
(A.Desirelli, 41-22-7678417, fax 41-22-7677910, alberto.desirelli@cern.ch)

Tests have also been performed on specimens extracted from the pure Al stabilizer of the CMS conductor. The tests were carried out at 4.2K, 77K and at room temperature for specimens in the as received and annealed conditions (thermal treated at 420°C – 1 h). Fig. 3 shows the stress strain curve for the annealed Al up to 1% strain. The calculation has been performed using the curve in Fig. 2. This curve, which corresponds to an annealed Al, has been used to check the maximum displacements and strains experienced by the winding throughout its working life. For the analysis presented here the assumption has been made that, after winding, the pure Al is in a state close to a stress-free strain-free state.

TABLE I
MATERIAL PROPERTIES AT 4.2 K

Material	Young's Modulus GPa	Poisson's ratio	Mean integral thermal expansion coefficient 293 K - 4.2 K K^{-1}
Al	see Fig. 2	0.33	$14.23\ 10^{-6}$
Al-alloy 2219	86	0.33	$14.16\ 10^{-6}$
Rutherford cable	90	0.33	$8.79\ 10^{-6}$
Fibre glass epoxy in the plane of the ribbon	23	0.37	$10.38\ 10^{-6}$
Fibre glass epoxy ⊥ to the plane of the ribbon	15	0.37	$20.77\ 10^{-6}$

B. Modelling of the Insulation

At low temperature, the first degradation occurring in the insulation is the failure of the matrix which, as it will be explained, is best seen as strain driven. For the insulation, which behaves in an elasto-brittle way, a criterion which takes into account the hydrostatic component of the stress tensor must be used. In our case the Mohr-Coulomb criterion has been adopted. According to this criterion, the calculated distribution of points (σ_{mean}, τ_{max}) must lay within an experimental failure envelope. If the material is isotropic the implementation of Mohr-Coulomb is straightforward. In the case of an orthotropic material, on the other hand, the use of this criterion is not trivial, due to the fact that the envelope is not univocal. One way around this problem is to consider the most restrictive envelope. However, since the scatter of the failure envelopes in terms of stress is greater than those in terms of strain, a strain based Mohr-Coulomb criterion should be used. It must be nonetheless pointed out that experimental evidence has shown a very low dependence of the modulus on fibre orientation [4]. The strain analysis using an underestimated modulus for the insulation will overestimate the strain in the insulation. This should provide a conservative indication of the working condition of the insulation. This technique requires the use of an experimental strain failure envelope. At present, the only experimental information available is relative to stress envelopes [5], [6]. So, even if not ideal, the results of the analyses are presented here in terms of stress. Further work is being carried out to determine the strain failure envelope by testing our samples at different shear/tension and shear/compression ratios. In each of the Mohr-Coulomb plots sown in Fig. 5, 7, 8, the 2 Mohr circles of the 2 most critical insulation locations, in terms of maximum compression and maximum tension, have also been traced. In Fig. 5, for example, the Mohr circle on the left intercepts the horizontal axis at a maximum compression value (σ_I) in excess of $1*10^8$ Pa. The Mohr circle on the right intercepts the horizontal axis at a maximum tension value (σ_{III}) a little below $1*10^8$ Pa. For the interfaces the results were extracted from the FEA in a form which could be compared with the experimental data available.

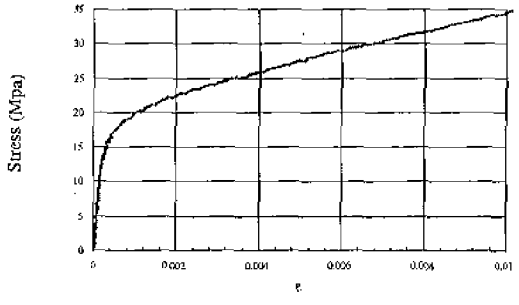

Fig. 3. CMS conductor Al stress strain curve Al 99.998% Annealed (420°C – 1 h), So = 6.01 mm^2, Lo=25.8 mm, T = 4.2 K, strain speed $3.3\ 10^{-4}\ s^{-1}$, E = 80 +- 3 GPa, Rp0.2 = 23 +4/-0 MPa, Rm = 294 -4/+0 MPa, εm = 46.7 %.

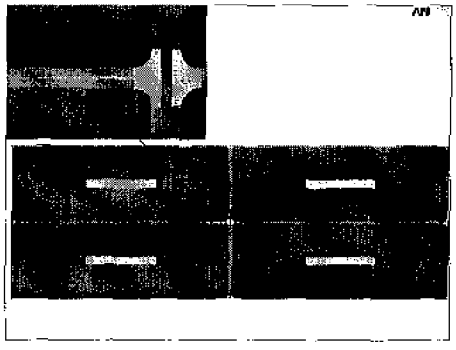

Fig. 4. The keystoning of the conductors

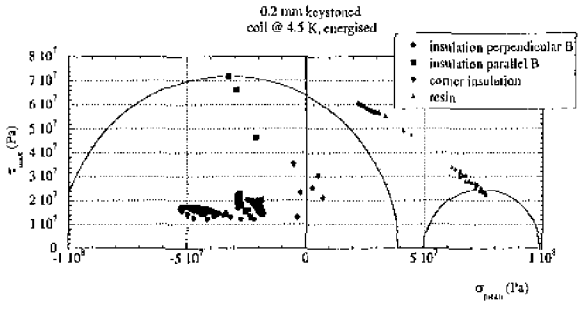

Fig. 5. Mohr-Coulomb plot for a keystoned conductor.

C. Keystoning of the conductor

The effect of the keystoning of the conductor was also modelled at INFN-Genova. The geometry of the keystoned conductor winding is shown in Fig. 4. The results of bending tests on sample lengths of conductor showed that the maximum keystoning was in the range of 0.2 mm. This might leave volumes of pure resin between turns. In order to avoid this and for many other practical reasons the insulation thickness on the conductor was increased to from 0.32 mm to 0.5 mm [2]. The results presented here are those for 0.5 mm insulation thickness. The Mohr-Coulomb plot in Fig. 5 shows the high stresses in the pure resin volumes.

III. The FE Modelling of the Suspension System

The support system has to ensure the suspension of the cold mass inside the vacuum tank. The loads seen by the suspension system are the 225 tonne weight of the cold mass and the magnetic forces due to coil misalignment relative to the yoke. The design takes into account the coil thermal contraction and the deflections due to magnetic forces. This study has been performed at CEA-Saclay using the software package Castem2000.

A. Description of the suspension system

The support system consists of a set of rods made of Ti-alloy *Ti-5Al-2.5Sn ELI (Extra Low Interstitial)*, see Table II. The longitudinal forces are taken by longitudinal tie rods. The weight and the radial forces are taken by 4 vertical tie rods and 8 tangential tie rods at 120° and 240° as shown in Fig. 6.

B. Load cases assessed

The study of the support system is made in 9 different cases:

- at room temperature: 300K
- at 300K, belt pre-stressed
- at cryogenic temperature and 0 field: 4K, 0T
- solenoid energised: 4K, 4T
- solenoid vertical misalignment
- solenoid horizontal misalignment in the x direction

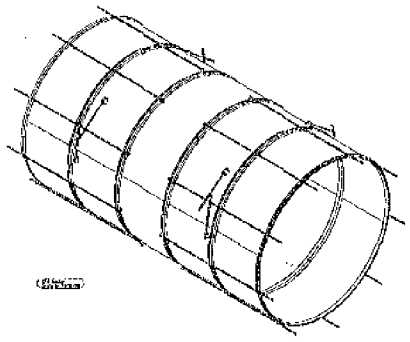

Fig. 6. The suspension system

TABLE II
Material Properties of *Ti-5Al-2.5Sn ELI* at 300 K and at 20 K

Material prop.	300 K	20 K
Young's Modulus [GPa]	110	130
UTS [MPa]	980	1500
Rp02 [MPa]	650	1150
Poisson's ratio	0.33	0.33
Mean integral thermal expansion coefficient 293 K - 4.2 K [K^{-1}]	3.1E-6 K^{-1}	

- solenoid horizontal misalignment in the z direction
- solenoid tilt misalignment around the x axis
- solenoid tilt misalignment around the y axis

IV. Results

The results are summarised in Tables III to IX and in Figures 7 and 8.

A. Coil at 4.5 K

In the load case of the Coil at 4.5 K the maximum Von Mises values found in the pure Al are in fact stress concentrations localised around the Rutherford cable (see Table III: Coil at 4.5 K , Pure Aluminium). Shear stress values at the interface between the pure Al stabilizer and the Rutherford cable (see Table V) are also well below the pull-out test ultimate value (35 MPa) [7]. The maximum hoop strain value is fairly evenly distributed across the whole Al cross section. The VM strain shows the peak values close to the Rutherford. A larger fraction of the Al cross section stays below 1.4‰. The stress field in the insulation appears to stay within the envelope values found in literature (see Table IV, Fig. 7 and Fig. 8: Coil at 4.5 K, coil end and coil centre) [5],[6]. For reasons of good legibility of the graphs, the experimental envelopes have not been included in Fig. 7 and Fig 8. In fact shear tests on CMS insulation have found shear failure values in excess of 100 MPa [6]. The envelope of the Mohr circles representing the stress state of the insulation in the lap shear sample is obviously only one part of the complete failure envelope of the material. Nonetheless, in this specific case, being the experimental values found so large, this portion of the failure envelope alone covers the area swept by the Mohr circles, representing the stress state

of the insulation within the coil. Radial and axial displacements of the coil at 4.5 K are shown in Table VI and Table VII.

B. *Coil at 4.5 K, energised*

Peak Von Mises stresses only increase by few MPa's when the magnet is energised. However, it must be noted that, in this load case, high Von Mises stress values appear all over the cross section of the Al-stabilizer (see Table III: Coil at 4.5 K - energised, Pure Aluminium). In this case too shear stress values at the interface between the pure Al stabilizer and the Rutherford cable (see Table V) are also well below the pull-out test ultimate value (35 MPa) [7].
As for the thermal load case the maximum hoop strain value is evenly distributed across the whole Al cross section. The VM strain of a large fraction of the Al cross section stays between 1.9 and 2.7‰. The stress field in the insulation is slightly increased by the energisation, but is still within the envelope values found in literature (see Table IV Fig. 7 and Fig. 8: Coil at 4.5 K, coil end and coil centre) [5],[6]. What pointed out about the failure envelope in the previous paragraph also applies here.
Radial and axial displacements of the coil at 4.5 K are shown in Table VI and Table VII.

C. *Suspension system*

In all the load cases assessed, the stresses in the suspension rods are below the allowed value.

TABLE III
VON MISES STRESS IN CONDUCTOR'S COMPONENTS

Material	Von Mises stress, Coil End [MPa]	Von Mises stress, Coil centre [MPa]
Coil at 4.5 K		
Pure Aluminium	4→20	4→20
SC Cable	138→169	138→168
Al alloy	0→66	0→66
Coil at 4.5 K, energised		
Pure Aluminium	13→20	15→22
SC Cable	71→139	17→128
Al alloy	51→97	115→145

TABLE IV
MAXIMUM SHEAR STRESS AT INSULATION–CONDUCTOR INTERFACE

Coil at 4.5 K	Shear stress [MPa]
Coil end location	54
Coil centre location	41
Coil at 4.5 K, energised	Shear stress [MPa]
Coil end location	54
Coil centre location	41

TABLE V
VON MISES AND SHEAR STRESSES AT INTERFACES (AL SIDE): COIL END/COIL CENTRE

Material Bonding	Max. Von Mises stress [MPa]	Max. Shear stress [MPa]
Coil at 4.5 K		
SC Cable ÷ Pure Aluminium	13→20 / 13→20	11 / 11
Pure Aluminium ÷ Al Alloy	4→15 / 4→15	8 / 8
Coil at 4.5 K, energised		
SC Cable ÷ Pure Aluminium	14→20 / 16→22	10 / 10
Pure Aluminium ÷ Al Alloy	13→17 / 16→18	8 / 7

TABLE VI
MAXIMUM VALUES OF RADIAL DISPLACEMENT

Coil at 4.5 K	Radial displacement (mm) Min	Max	**Coil at 4.5 K, energised**	Radial displacement (mm) Min	Max
Coil end location	-14.9	-13.4	Coil end location	-12.8	-10.9
Coil centre location	-14.7	-13.4	Coil centre location	-10.0	-8.5

TABLE VII
MAXIMUM VALUES OF AXIAL DISPLACEMENT

Coil at 4.5 K	Axial displacement (mm) Min	Max	**Coil at 4.5 K, energised**	Axial displacement (mm) Min	Max
Coil end location	-26.5	-25.8	Coil end location	-31.2	-30.0
Coil centre location	-0.7	-0.6	Coil centre location	-0.8	0

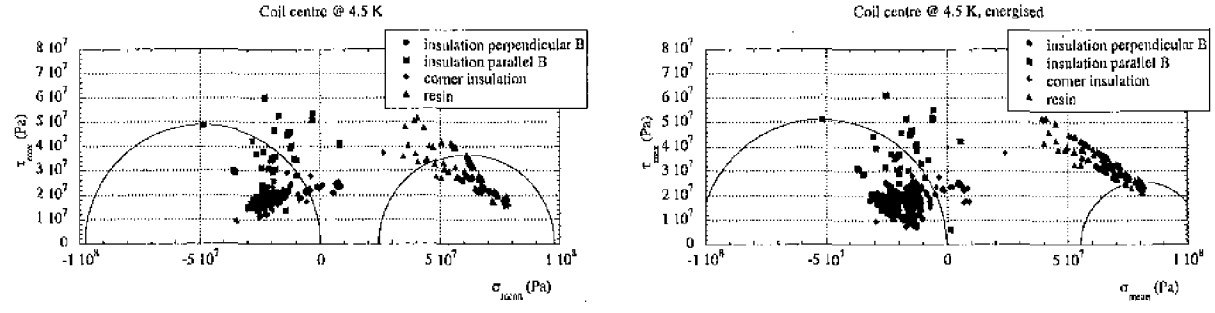

Fig. 7. Coil centre location - (σ_{mean}, τ_{max}) distribution in the insulation.

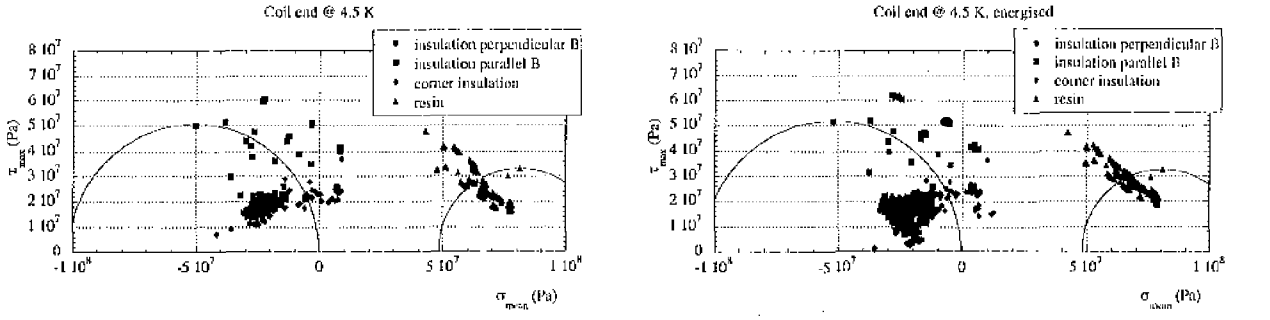

Fig. 8. Coil end location - (σ_{mean}, τ_{max}) distribution in the insulation.

V. Conclusions

A. Insulation

Cool down gives the largest contribution to the stress field in the insulation, on the other hand the effect of the EM forces seems to be relatively small. Another important issue is the one of possible pure resin volumes in the winding. These volumes may be present either between the insulation of two or four conductor corners or in the inter-turn gaps due to the keystoning of the conductor. For this as well as for practical reasons it was decided, following a study carried out by INFN-Genova to increase the insulation thickness.

B. Aluminium

The pure Al stabilizer is well into the plastic domain. The present conductor geometry has been chosen to minimise most of the structural function of the pure Al.

C. Al-alloy

The stresses in the Al-alloy too appear to be below the allowable values.

D. Suspension system

In all the load cases assessed, the stresses in the suspension rods and longitudinal tie rods are below the allowed value.

Acknowledgement

The authors would like to thank, Pascal Petiot and Carnita Hervet for their help in the document and poster preparation.

References

[1] A. Hervé, "The CMS detector magnet," *MT-16*.
[2] P. Brédy, A. Calvo, B. Curé, D. Campi, A. Desirelli, P. Fabbricatore, S.Farinon, A. Hervé, S. Horvath, F.Kircher*, V. Klioukhine, B. Levesy, M. Losasso, J.P.Lottin, R. Musenich, Y. Pabot, A. Payn, C. Pes, C. Priano, F. Rondeaux, S.Sgobba, "Final design of the CMS solenoid cold mass" *MT-16*.
[3] B. Gallet, "Essais mécaniques sur l'aluminium du conducteur ALEPH-VAC, CEA," *Report No DSM DAPNIA STCM 276TC02*.
[4] A. Desirelli, B. Gallet, F. Kircher, J.M. Rey, "Failure criterion of glass/epoxy composites as electrical insulation for large SC magnets," *I.C.M.C. Portland, Oregon, U.S.A. 28 July - 1 Aug. 1997*
[5] D.F. Baynham, D. Evans, S.J. Gamage, R.J.S. Greenhalgh, D. Morrow and S.J. Robertson, "Transverse mechanical properties of glass reinforced composites," *Report CLRC: AECT/70/96 Nov. 1996*
[6] B. Levesy, "Shear test of glass reinforced composite materials at 4K" *MT-16*.
[7] S. Horvath, Private communication.
[8] A. S. Khan, S. Huang , "Continuum theory of plasticity" *John Wiley &Sons, Inc. ISBN 0-471-31043-3*.